Journal of Applied Polymer Science

Carbon Nanotubes-Filled Thermoplastic Polyurethane–Urea and Carboxylated Acrylonitrile Butadiene Rubber Blend Nanocomposites

Nasir Mahmood,[1,2] Asad Ullah Khan,[2] Klaus Werner Stöckelhuber,[3] Amit Das,[3] Dieter Jehnichen,[3] Gert Heinrich[3,4]

[1]Institut für Chemie, Fachgruppe Mikro- und Nanostrukturbasierte Polymerverbundwerkstoffe, Martin-Luther-Universität Halle-Wittenberg, D-06120 Halle (Saale), Germany

[2]Department of Chemical Engineering, COMSATS Institute of Information Technology, 54000 Lahore, Pakistan

[3]Institut für Polymerwerkstoffe, Leibniz-Institut für Polymerforschung Dresden e.V., D-01069 Dresden, Germany

[4]Institut für Werkstoffwissenschaft, Technische Universität Dresden, D-01069 Dresden, Germany

Correspondence to: N. Mahmood (E-mail: nmahmood@ciitlahore.edu.pk)

ABSTRACT: This article reports the preparation and characterization of multiwalled carbon nanotubes (MWCNTs)-filled thermoplastic polyurethane–urea (TPUU) and carboxylated acrylonitrile butadiene rubber (XNBR) blend nanocomposites. The dispersion of the MWCNTs was carried out using a laboratory two roll mill. Three different loadings, that is, 1, 3, and 5 wt % of the MWCNTs were used. The electron microscopy image analysis proves that the MWCNTs are evenly dispersed along the shear flow direction. Through incorporation of the nanotubes in the blend, the tensile modulus was increased from 9.90 ± 0.5 to 45.30 ± 0.3 MPa, and the tensile strength at break was increased from 25.4 ± 2.5 to 33.0 ± 1.5 MPa. The wide angle X-ray scattering result showed that the TPUU:XNBR blends were arranged in layered structures. These structures are formed through chemical reactions of —NH group from urethane and urea with the carboxylic group on XNBR. Furthermore, even at a very low loading, the high degree of nanotubes dispersion results in a significant increase in the electrical percolation threshold. © 2014 Wiley Periodicals, Inc. J. Appl. Polym. Sci. **2014**, *131*, 40341.

KEYWORDS: blends; nanotubes; graphene and fullerenes; rubber; polyurethanes; elastomers

Received 19 July 2013; accepted 21 December 2013

DOI: 10.1002/app.40341

INTRODUCTION

A number of materials are known, which find applications as reinforcing fillers for plastics and rubbers. Reinforcing fillers are usually selected from particulate carbon blacks and certain inorganic compounds. Fibrous materials are also used in rubber compounds to improve various properties. These materials may include cellulose[1,2] fibers, glass fibers,[3] and synthetic organic fibers, such as melamine,[4,5] aramid fiber, and so forth.[6] However, with the discovery of carbon nanotubes (CNTs), considerable attention has been paid on the CNT containing composites.[7] It is because of the fact that CNT consist of rolled-up graphene sheet built from sp^2 carbon structure.[8,9] These are considered as ideal reinforcing fillers in a wide range of composite systems.[10] This is due to their high aspect ratio and superior Young's modulus (1–1.8 TPa) as compared to the other fibrous fillers. Their electrical properties (resistivities at 300 K of $\sim 1.2 \times 10^{-4} - 5.1 \times 10^{-6}\Omega$·cm; activation energies <300 meV for semiconducting tubes) and thermal conductivity (300 W/m·K) make them suitable for electrically conducting materials.[11–16] The most important commercial application of multiwalled CNTs (MWCNTs) is traced back as electrically conducting components in polymer composites. The polymer matrix of a composite also plays an important role in achieving desirable electrical conductivities, that is, 0.01–0.1 S cm^{-1}. The composites with this range of conductance can be obtained with a 5% by weight loading of the MWCNTs.[10] In fact, the mechanical strength is increased in addition to the increase in the electrical conductivity. The fibrous morphology and the low loading of the MWCNTs make it possible to achieve the desired electrical conductivity value without compromising the other properties such as mechanical properties and the low melt flow viscosity.

To obtain a superior quality composite material, it is very important to disperse the nanotubes uniformly and also to achieve maximum nanotube–matrix adhesion. The dispersion of the CNTs in the polymer matrix is quite cumbersome task for preparing reinforced nanocomposite. It is because of the fact that the CNTs in their manufactured state are held together by strong van der Waal's attractive forces. However, the CNTs need

Table I. Formulation of the Rubber Blend Mixes

S. no.	Rubber recipe	Amount (phr[a])
1	XNBR	80
2	TPUU	20
3	ZnO	2.4
4	*N*-Cyclohexyl-2-benzothiazolsulfanamid (CBS)	1.36
5	Stearic acid	1.6
6	Sulfur	1.12

Two types of samples were used; one containing 1, 3, and 5 wt % of CNTs of the XNBR:TPUU contents, the other was without CNTs.
[a] Parts per hundred of rubber.

to be dispersed uniformly in the polymer matrix, so that the composite material has superior properties. It is well-known that the nanotube reinforced polymers have excellent properties; however, poor dispersion of the CNTs limits the enhancement of the properties. The presence of entanglements or aggregates within the CNTs is one factor that strongly influences the dispersion. Yao and Manas-Zloczower[17] have successfully used two roll mill for the dispersive mixing and have concluded that the shear stress distribution in the material and the elongated flow component provides better mixing. In another study, Kim et al.[18] have used the roll mill to prepare aligned CNTs-filled rubber composites. It has been reported that the dragged shear forces are the cause of the CNTs dispersion in the rubber matrix.

In the present work, we report for the first time, the preparation and characterization of the MWCNTs (called here after CNTs)-filled thermoplastic polyurethane–urea (TPUU):carboxylated acrylonitrile butadiene rubber (XNBR) blend nanocomposites. These are very unique blends and have been recently reported by the authors.[19] The mixing of the CNTs was carried out using a laboratory two roll mill. The amount of the CNTs used was 1, 3, and 5 wt % of the blend sample. To validate the application of the CNTs in such blend system, a variety of properties like tensile strength, dynamic-mechanical, electrical conductivity, the morphology, and so forth were investigated. The properties of the filled elastomer blend nanocomposites are compared with those of the unfilled one.

EXPERIMENTAL

Materials

Carboxylated acrylonitrile rubber (XNBR Krynac X 740) was obtained from Lanxess, Germany. CNTs used were of unmodified commercial grade obtained from Nanocyl S.A (Nanocyl 7000), Sambreville, Belgium, of having average diameter: 10–20 nm and length: 1.5 μm. Zinc oxide, stearic acid, *n*-cyclohexyl-2-benzothiazole-sulfenamide, and soluble sulfur used in this study were of industrial grades and used without any purification. Analytical grade tetrahydrofuran (THF) was obtained from Sigma-Aldrich and used as obtained. The TPUU used in this study were prepared by reacting 4,4′-diphenylmethane diisocyanates with a poly(tetramethylene carbonate)diol in presence of 1,2-di(*p*-aminophenoxy)ethane as chain extender. The reactants for preparing the TPUU were acquired from Sigma-Aldrich.

Preparation of TPUU and XNBR Blends

The rubber blends and the blend nanocomposites were prepared using a two-step procedure. The formulation details are given in Table I. In the first step, the TPUU and XNBR were dissolved in THF to obtain a homogeneous solution. The dissolved components were further blended at a temperature of 50°C for a period of 2 h in an ultrasonication bath. The CNTs-filled blend nanocomposites were prepared by adding 1, 3, and 5 wt % of the CNTs to the solution-mixture followed by ultrasonication for 15 min to enhance the dispersion. The mixture was then dried in a vacuum oven at 50°C for 12 h to ensure the complete removal of THF. Finally, the additives such as zinc oxide, stearic acid, organic accelerators, and sulfur were added using a two roll mill (Polymix 110L, size: 203 × 102 mm^2, Servitech GmbH, Wustermark, Germany). Afterward, by controlling the milling conditions (i.e., nip gap 0.5–0.3 mm, mixing time, temperature 60°C), the dispersion of the CNTs in blend matrix was accomplished by shear and elongational forces.

Curing studies were performed using a rubber processing analyzer Scarabaeus SIS V50 in an isothermal time-sweep mode at 150°C for 60 min. To minimize the reorientation process of the CNTs, the sheets obtained from roll mill were vulcanized in a compression molding machine at 150°C for 30 min by strictly following the milling direction.

Measurements

Scanning Electron Microscopy. Morphology of the blend nanocomposites was determined with the help of (LEO 435) scanning electron microscope (SEM—acceleration voltage 20 kV) manufactured by LEO Electron Microscopy Limited, Cambridge, England. The cryogenically fractured elastomeric composites were used for the dispersion analysis of the TPUU in the XNBR matrix.

Transmission Electron Microscopy. The high-resolution transmission electron microscope (HR-TEM) images were obtained on a (JEOL 2100) TEM. For the HR-TEM observation, ultrathin sections of the specimens were obtained at −80°C in liquid nitrogen using a Leica Ultracut UCT ultramicrotome equipped with a diamond knife. The ultrathin cuts were obtained from the samples as described in Figure 1. The thickness of the HR-TEM specimens was approximately 80 nm. These specimens were then placed on the copper grid for the image analysis.

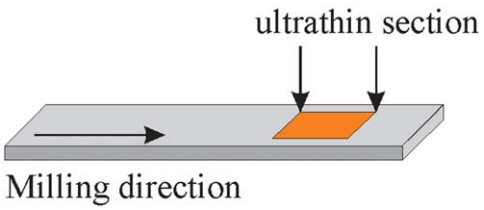

Figure 1. A schematic representation for the preparation of TEM samples. [Color figure can be viewed in the online issue, which is available at wileyonlinelibrary.com.]

Mechanical Properties. Stress–strain behavior of the TPUU/XNBR blend and the blend nanocomposites was determined according to ISO 527 method at a cross-head speed of 200 mm/min using a tensile testing machine from Zwick GmbH, Ulm, Germany.

Dynamic-Mechanical Thermal Analysis. Dynamic-mechanical thermal analysis (DMTA) was performed on the rectangle strips of dimensions 10 × 1 × 35 mm^3, using a dynamic-mechanical thermal spectrometer (Gabo Qualimeter, Germany, model Eplexor-150N) in the tension mode at a temperature range from −60 to 100°C. The isochronal frequency used was 10 Hz and the heating rate was 2 K min^{-1}. Amplitude sweep experiment was carried out on Gabo Qualimeter (Germany, model Eplexor-2000N) at room temperature. For this experiment, tension mode was selected for the variation of the dynamic load from 0.01 to 100% at 10 Hz frequency. A prestrain of magnitude 10% was chosen to hold the sample with the size of 10 × 1 × 35 mm^3.

Wide Angle X-Ray Scattering. The wide angle X-ray scattering (WAXS) patterns for the neat TPUU, XNBR, and CNTs-filled blend nanocomposites were measured using an X-ray diffractometer (XRD 3003 T/T,GE Sensing & Inspection Technologies GmbH, Vertriebs zentrum SEIFERT-FPM Freiberg/Saxony, Germany) with Cu-Kα radiation (40 kV, 30 mA, monochromatization by primary multilayer system) in the scattering range: $2\theta = 5°–40°$ in transmission ($\omega/2\theta = 1{:}2$ and step-scan mode: measuring time $\Delta t = 15$ s for each point and the $\Delta 2\theta = 0.05°$).

Conductivity Measurement. The volume conductivity was measured according to standard ISO 1853:2011. The sample of rectangular geometry with dimensions of approximately 140 × 50 × 2 mm (length × width × thickness). The resistances were measured with a Sefelec teraohmmeter MP1500P. The voltage used in the measurements was 10 V.

RESULTS AND DISCUSSION

The preparation and characterization results of the unfilled TPUU:XNBR blends are communicated by the authors elsewhere.[19] It is important to mention that such blend systems have unique mechanical properties due to their good compatibility. To extend their application range, in the prevailing study, the results on the preparation of CNTs-filled blend nanocomposites are reported. The blend ratio used in this study was 80 parts XNBR and 20 parts TPUU.

The CNTs-filled TPUU:XNBR blend nanocomposites were prepared by following two-step approach as described in the Experimental section. It is well established that ultrasound sonication is one of the favorable approaches to disperse thoroughly the nanoparticles into the matrix.[20] Therefore, in the present study, to enhance the dispersion of the CNTs in the TPUU:XNBR solution mixture sonification was carried out. In the second step, the mixture was mixed on a laboratory two roll mill, by controlling the milling conditions, that is, the nip gap, the mixing time, and temperature conditions, that is, 60°C. During two roll mill mixing, the elongational shear stresses make the mixing material to form a continuous matrix and as a result the shear flow maximizes the dispersion as well as the alignment of the filler in the direction of the shear force. In the present work, the same concept has been applied for dispersion of the CNTs, and the obtained results are discussed in the following part.

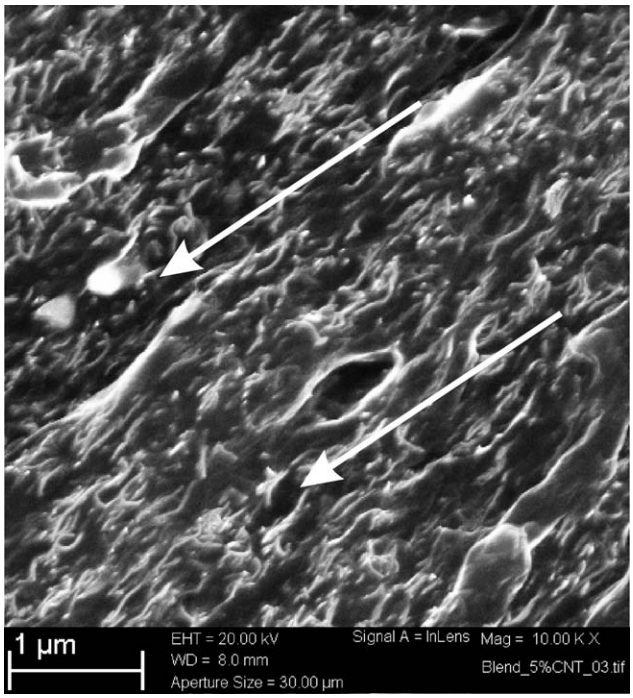

Figure 2. SEM image of the filled blend nanocomposite filled with 5 wt % of the CNTs. Arrow shows the direction of the shear flow.

To quantify the state of dispersion of the CNTs in the TPUU:XNBR blends, the nanocomposites were examined using the SEM and HR-TEM. Figure 2 shows the SEM of a cryofractured sample filled with 5 wt % of CNTs. An overview of the two roll mill mixing effect on the dispersion of the CNTs in the blends can be observed from the figure. From the image, it is evident that the TPUU phase has elongated along the shear flow direction. This happen due to the softening of the TPUU phase during two roll mill mixing at 60°C temperature conditions and, therefore, the applied shear forces distribute and as a result the TPUU phase elongate in the flow direction. Also, at the same time, the softened TPUU phase contributes as a soft phase in the blend system. This further enhances the possibility of evenly dispersion of the CNTs during mixing. It can also be observed from the SEM micrographs that the CNTs are also distributed as the TPUU phase. This happens because of the distribution of the shear and the elongational forces during two roll mill mixing.

Further confirmation of the CNTs dispersion can be made through TEM analysis. The TEM images for the blends containing 3 and 5 wt % CNTs are shown in Figure 3(a,b). In these TEM images, it is clearly visible that no aggregates of the CNTs can be observed. The dispersion of the CNTs in the blend matrix is quite impressive. The CNTs are mostly dispersed along the shear flow direction and are distributed as individual tubes. After comparing the images, it becomes evident that the shear flow influences the dispersion of the CNTs. As indicated by circles in the figure that CNTs are preferentially distributed in

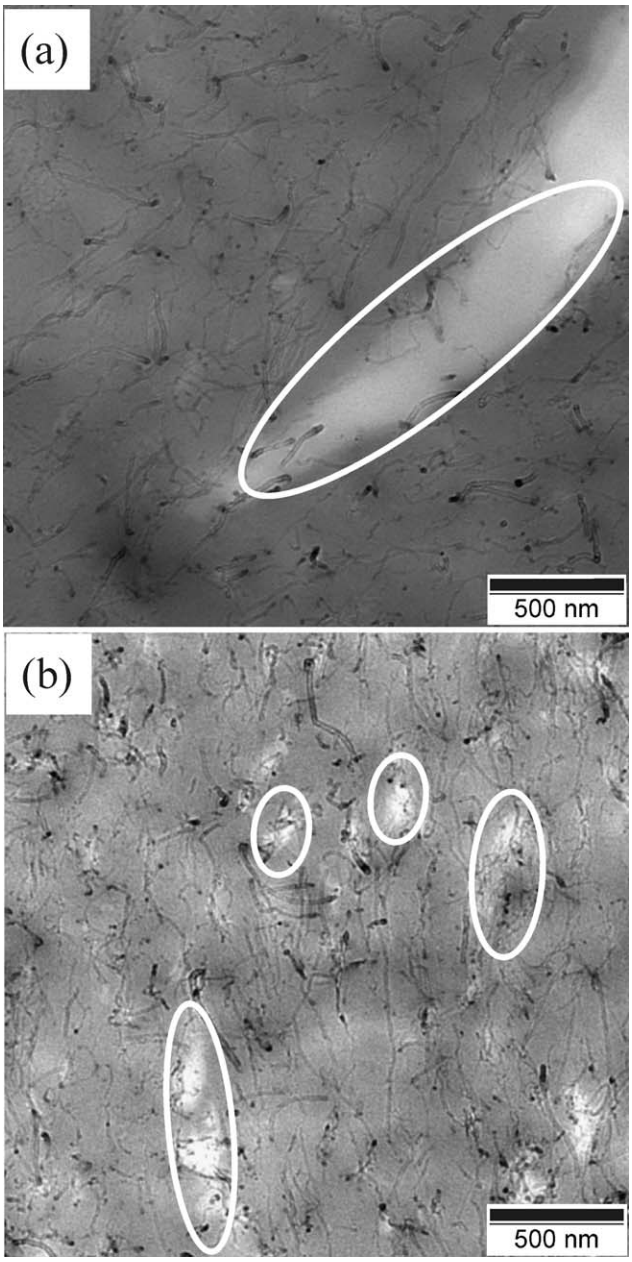

Figure 3. TEM images of the blend nanocomposite filled with: (a) 3 wt % and (b) 5 wt % of the CNTs. The encircled portions in the images indicate the TPUU phase of the blend system.[19]

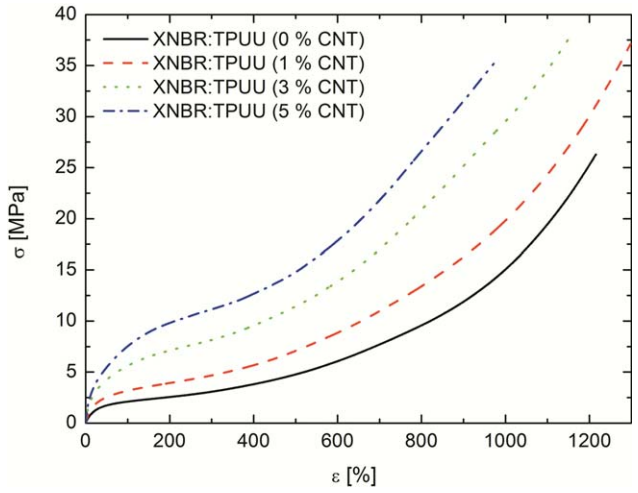

Figure 4. Comparison plot of tensile strength vs. elongation of the unfilled and filled XNBR:TPUU blend nanocomposites. [Color figure can be viewed in the online issue, which is available at wileyonlinelibrary.com.]

the XNBR phase of the systems. However, in the samples with 5 wt % of the CNTs, they are also present in the TPUU phase. This clearly shows that the CNTs have more preference to the XNBR phase of the blend system. The SEM and TEM image analysis confirms the utility of the two roll mill mixing for preparing well-dispersed CNTs-filled novel TPUU:XNBR blend nanocomposites.

To investigate the effect of nanotubes on the physical properties of the blends, tensile, dynamic-mechanical, and the electrical conductive properties were measured and compared with the unfilled blends. In Figure 4, the stress–strain plot of the TPUU:XNBR blends and their corresponding blend nanocomposites is shown. The addition of the CNTs causes an enhancement of the mechanical properties of the TPUU:XNBR blends. The data trend shows that the mechanical properties increase significantly with increasing the amount of the CNTs in the blend. The well-dispersed CNTs in the blend effectively absorb the applied stress and to improve the mechanical stiffness of the corresponding nanocomposite. These experimental results clearly indicate that the incorporation of the CNTs into such blends have significantly improved their mechanical properties in comparison to the neat one.

Table II lists the mechanical properties data averaged from five measurements on the unfilled blend and its corresponding

Table II. Mechanical Properties: "Elastic Modulus (E_t), Stress (σ), Stress at Break (σ_B), and Strain at Break (ε_B)," of Thermoplastic Polyurethane-Urea and Carboxylated Nitrile Butadiene Rubber Blend and CNTs-Filled Blend Nanocomposites

	Properties			
Sample type	E_t (MPa)	σ 300% (MPa)	σ_B (MPa)	ε_B (%)
XNBR:TPUU (0 wt % CNTs)	9.9 ± 0.5	3.0 ± 0.11	25.4 ± 2.5	1215 ± 50
XNBR:TPUU (1 wt % CNTs)	17.9 ± 1.0	4.8 ± 0.2	35.9 ± 1.0	1295 ± 18
XNBR:TPUU (3 wt % CNTs)	32.0 ± 1.5	8.2 ± 0.2	35.4 ± 0.5	1150 ± 20
XNBR:TPUU (5 wt % CNTs)	45.3 ± 0.3	11.2 ± 0.3	35.0 ± 1.5	1000 ± 35

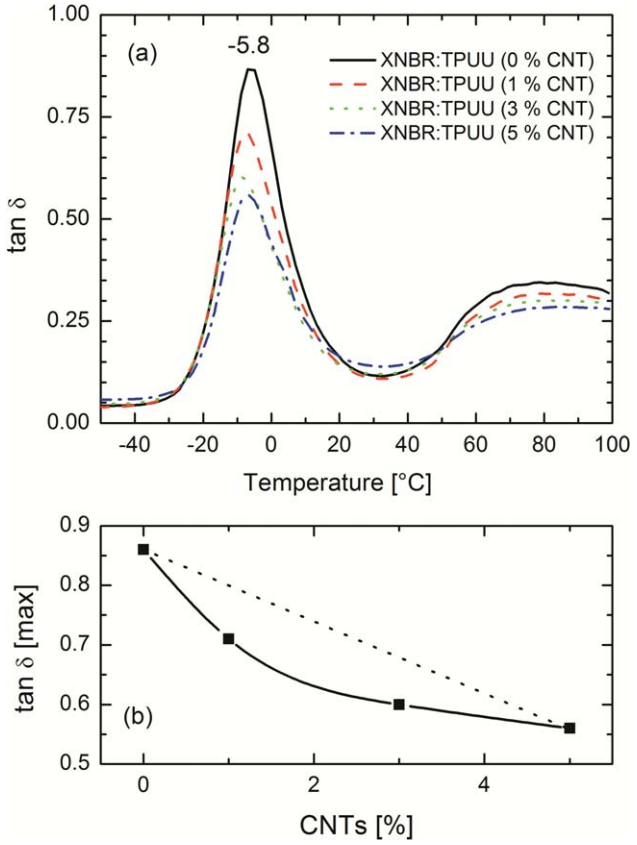

Figure 5. (a) Temperature dependence of tan δ for the neat TPUU/XNBR and the blend nanocomposites containing 1, 3 and 5 wt % of CNTs. (b) tan δ intensity (maximum) plot against samples with different wt % of CNTs. [Color figure can be viewed in the online issue, which is available at wileyonlinelibrary.com.]

CNTs-filled blend nanocomposites. The addition of the CNTs causes an enhancement of the mechanical properties of the blend. It shows that the modulus increase significantly with the addition of the CNTs; however, the elongation at break is decreased as the CNTs contents are increased. The sample with 1% CNTs has higher elongation at break compared to the neat blend sample. This could be explained by considering the distribution of CNTs depicted in TEM image (Figure 3a). It is clearly evident from the image that the CNTs are mainly distributed in the XNBR phase. Such a distribution of the CNTs in blend matrix makes the TPUU phase more ductile and, therefore, the sample with less CNTs show higher strain at break. However, for the sample with higher CNTs loading, the strain at break has decreased and the effect at 5% is more pronounced. In the TEM image shown in Figure 3b with 5% CNTs, it is clearly evident that the CNTs are distributed in the TPUU phase as well. This could be the reason that the stiffness of the samples has decreased as result the lower strain at break is observed. These experimental results clearly indicate that the introduction of the CNTs in the blends make significant improvements in their mechanical properties. An important conclusion drawn from the tensile results is that CNTs-filled blend nanocomposites that show higher tensile (elastic modulus, strain at break) properties compared to the unfilled blend is due to well-distributed CNTs.

The influence of CNTs incorporation on the loss tangent (tan δ) of TPUU:XNBR blend system over a temperature range of -60 to 100°C at a frequency of 10 Hz is depicted in Figure 5a. As expected, the intensity of the tan δ peak decreases with increasing the amount of the CNTs in the blend system. It can also be observed from the figure that on addition of the CNTs there is no significant shift of the tan δ peak at about -5.8°C. Such an observation clearly excludes a possibility of chemical interaction between the matrix and the CNTs. However, a large variation in shape and intensity of the tan δ peaks for the blend samples with different CNTs loading suggests that the extent of interaction/distribution of the CNTs affects this largely. Maiti et al.[21] have quantitatively estimated the filler distribution in immiscible rubber blend systems and related this to the intensity of the tan δ peak at T_g of the phases. A linear correlation in decreasing the intensity of tan δ peaks with different amount of filler loading suggests an even distribution of the filler in the rubber blend systems.[21] The same concept has been used to explain the CNTs distribution in the TPUU:XNBR blend system. To follow this, the intensity values of the tan δ peak taken from the data shown in Figure 5a are plotted in Figure 5b against samples with different CNTs wt %. The decrease of the tan δ intensity deviates from linear behavior for samples with 1 and 3 wt % CNTs, this clearly indicates that the CNTs are not

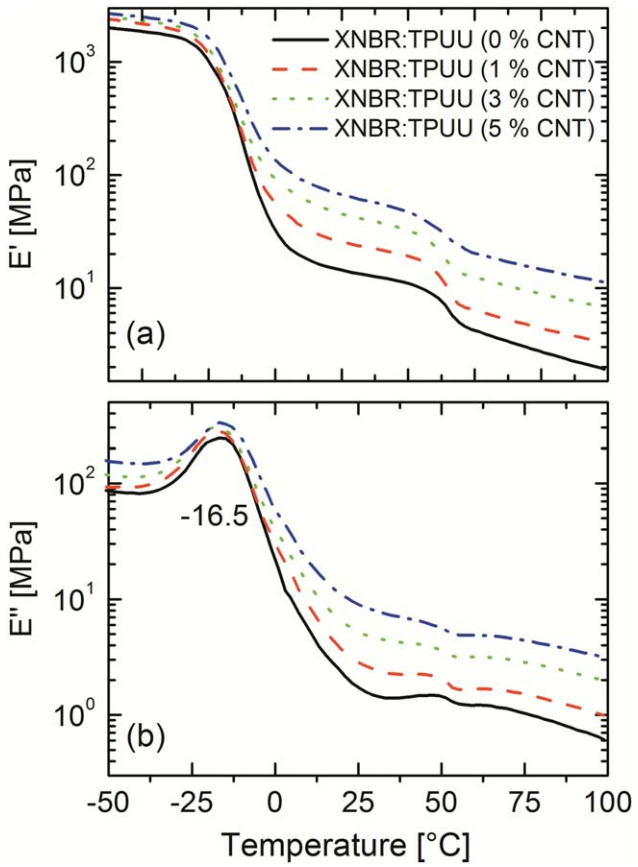

Figure 6. Temperature dependence of the storage (a) and loss (b) moduli for the neat TPUU/XNBR and the blend nanocomposites containing 1, 3, and 5 wt % of CNTs. [Color figure can be viewed in the online issue, which is available at wileyonlinelibrary.com.]

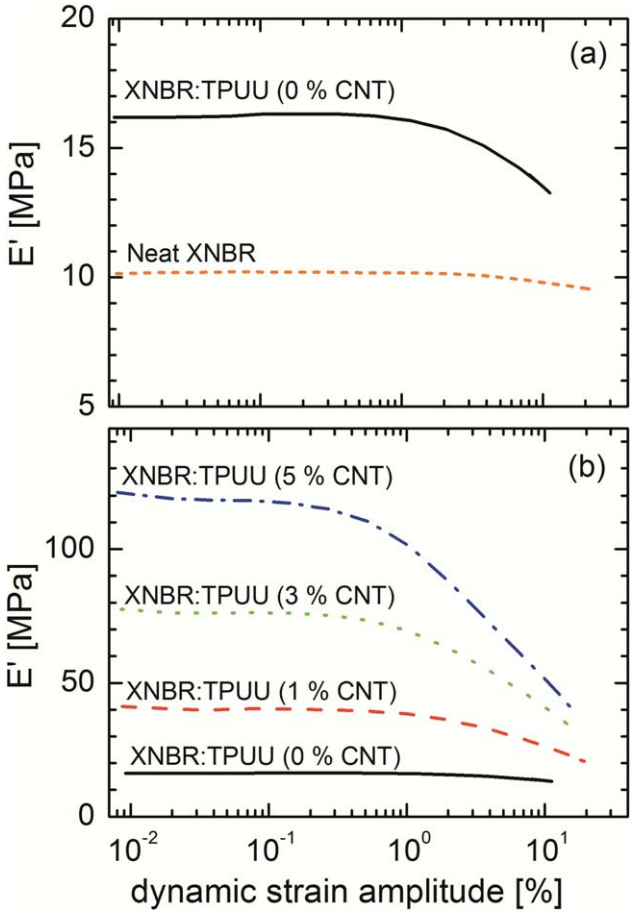

Figure 7. Dynamic strain amplitude plot for the neat rubber, TPUU:XNBR blend and the blend nanocomposites containing 1, 3, and 5 wt % of CNTs. Frequency used was 10 Hz. In figure (a), data for neat blend and XNBR are shown at smaller scale for comparison purpose. [Color figure can be viewed in the online issue, which is available at wileyonlinelibrary.com.]

distributed evenly in both the blend phases. It is more likely that they distribute in XNBR phase of the blend system preferentially and because of this reason a nonlinear behavior in decrease of the tan δ intensity is observed. However, with increasing the amount of the CNTs in the blend system, this becomes linear when compared with unfilled blend. This may be attributed that the CNTs are also distributed in the TPUU phase and hence results in a linear decrease of tan δ intensity.[22,23]

The nanocomposites have higher storage modulus below and above the T_g of the unfilled blend sample (see Figure 6a). Above 0°C, the storage modulus decrease steadily with a transition observed between 44 and 55°C, where it changes abruptly to lower values. This decrease in modulus is mainly due to the melting of a phase, probably the hard segments in the TPUU, which takes place at 44.7°C.[19] However, with increasing the amount of CNTs, this change in the modulus (E') becomes nearly linear, indicating that the CNTs are also distributed in the TPUU phase. A system with well-dispersed CNTs in both the blend phases is expected to exhibit slow relaxation behavior of the TPUU phase in comparison to the system, where mainly CNTs are largely located in XNBR phase (refer Figure 3a). As a result, the transition observed between 44 and 55°C become less pronounced for a sample with higher amount of the CNTs. Conversely, the location and intensity of the E″ peaks, which reveal only the segmental motion of the low glass transition components in the blend system, are not appreciably influenced by the CNTs loading (Figure 6b).

The difference between the filled and the unfilled blend can also be observed through the linear viscoelastic strain sweep experiment. In a strain sweep experiment, the amplitude is changed, whereas the frequency of the dynamic mechanical analyzer (DMA) is kept constant. In these experiments, a frequency of 10 Hz was used. This in general reveals the state of the filler network, and the breakdown of this network is induced by the

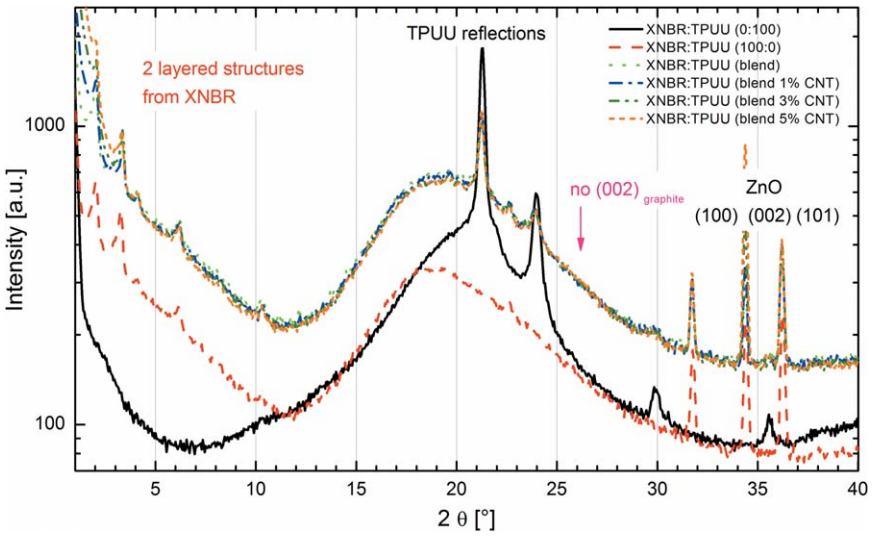

Figure 8. WAXS 2 theta-plot for the neat TPUU, XNBR, neat blend, and the blend nanocomposites containing 1, 3, and 5 wt % of CNTs. [Color figure can be viewed in the online issue, which is available at wileyonlinelibrary.com.]

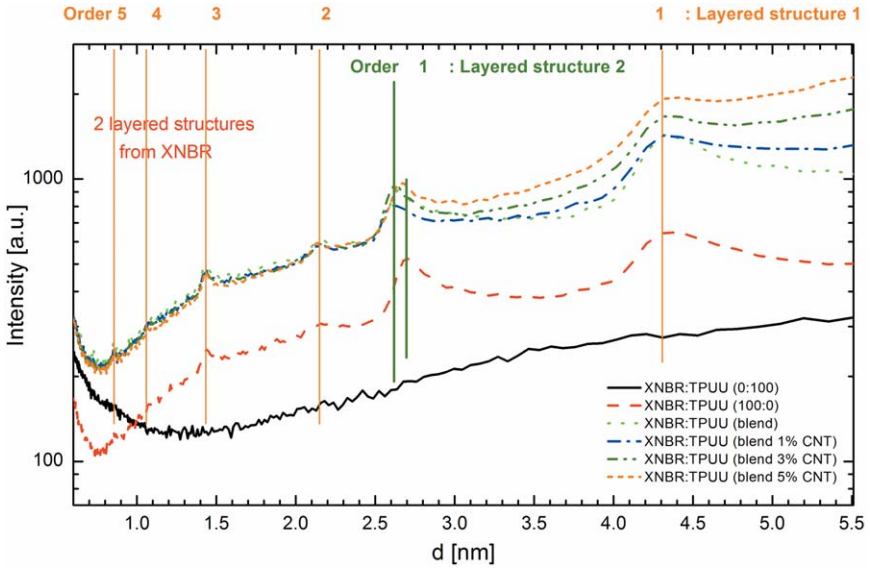

Figure 9. WAXS *d*-plot for the neat TPUU, XNBR, neat blend, and the blend nanocomposites containing 1, 3, and 5 wt % of CNTs. [Color figure can be viewed in the online issue, which is available at wileyonlinelibrary.com.]

increase in the amplitude of deformation during the dynamic-mechanical experiment. From Figure 7a, it can be observed that the blend sample (TPUU:XNBR) shows slightly higher storage modulus (E') compared to the neat rubber (XNBR). This increase of E' can be explained as follows: TPUU urethane/urea–NH group reacts with the carboxylic group of the XNBR phase to form amide linkage,[19] the urethane/urea/amide segments aggregate into microdomains resulting in a structure consisting of glassy, hard domains, and the rest blend phase act as the soft one. The hard domains gain their rigidity through physical crosslinking (hydrogen bonding between them) and provide filler-like reinforcement to the soft blend phase. Because of this reason, slightly higher E' is observed for TPUU/XNBR blend in comparison to the neat vulcanized XNBR rubber. In case of the CNTs-filled blend nanocomposites (Figure 7b), there is large increase of the E', which shows that the CNTs are well-dispersed and form a network structure.

It is important to see, that as the content of the CNTs is increased in the blends, the E' value increases significantly. Only 5 wt % of the CNTs in blends leads to a fivefold increase of E' when compared with the unfilled blend, confirming the idea of well-dispersed CNTs in the blend system.

Figure 8 shows the X-ray diffraction pattern for the neat and the CNTs-filled samples. The curves for the filled samples are very similar. A set of reflections observed in the lower angles is mainly from XNBR phase and in the central area caused by the TPUU phase of the blend system. At higher angle, the reflections are due to the ZnO used in the formulation. However, no reflection is observed at graphite reflection angle, that is, $2\theta \sim 26^\circ$. A significant change in the scattering behavior could not be found that might be the result of good compatibility of the blend phases. The TPUU reflections at higher angles, that is, $2\theta = 29.9^\circ$ and 35.5° are clearly reduced in the blend systems. This could be the result of the reaction of TPUU and the XNBR resulting in compatible blend system. Furthermore, a small orientation of the reflections of ZnO is visible from the figure (variable ratios in between the reflections measured).

The layered structure can be characterized by the interlayer spacing, which is plotted in Figure 9 for the different samples. The layered structure is observed only for the samples having XNBR component in both filled and unfilled samples. One type of the structure with a layer distance of ~4.30 nm can be observed up to the fifth reflection order and the other appears at ~2.62 nm. However, for neat XNBR, the structure of a layer distance is observed at ~2.70 nm. A slight decrease in layer spacing for blend system could be the result of the reaction of TPUU phase with the XNBR, where urea and urethane–NH group, react with the carboxylic functional group of XNBR to form an amide linkage.[19]

The direct current (DC) electrical percolation behavior of the nanocomposites is shown in Figure 10. It is evident from this figure that there is a sharp rise of conductivity, when the CNTs

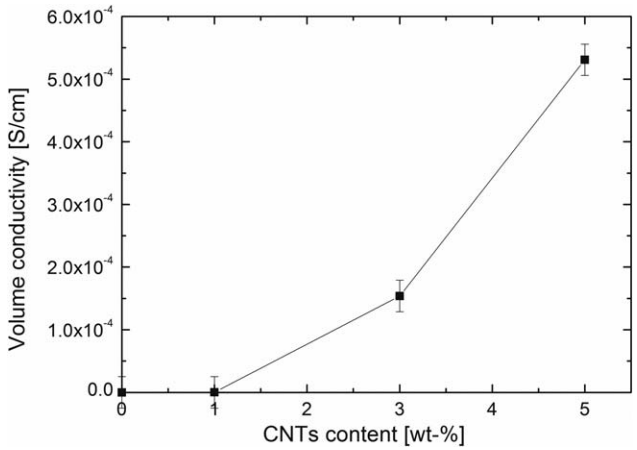

Figure 10. Dependence of DC electrical conductivity on the CNTs content of TPUU:XNBR blend nanocomposite.

amount is increased from 1 to 5 wt %. This rise in conductivity is caused by the formation of a continuous network of the CNTs. The very high aspect ratio and good dispersion of the CNTs is mainly responsible for this percolation behavior even at very low loadings. Therefore, it can be concluded that the dispersion of CNTs in such blend systems can be achieved using the two roll mill. As a result of the two roll mill mixing, the formation of the CNTs network with a smaller amount is achieved, that gives rise to the DC electrical conductivity.

CONCLUSIONS

Nanocomposites of XNBR:TPUU blend containing different weight fractions of CNTs were prepared and characterized. The dispersion of CNTs in the XNBR:TPUU blend was carried out in a two roll mill and characterization was conducted by WAXS, DMTA, mechanical property testing (stress–strain behavior), SEM,***** and TEM. It has been found that CNTs are well-dispersed in the matrix mainly in the XNBR phase. The incorporation of the CNTs resulted in an increase in the mechanical properties to a significant extent of the TPUU:XNBR blend. WAXS study indicates that layered structures are observed for the samples having XNBR component in both filled and unfilled samples. Furthermore, the DC conductivity measurement indicates that the presence of even a very small weight percent of well-dispersed MWCNTs, results in a significant increase in the electrical percolation threshold.

ACKNOWLEDGMENTS

Financial and research support by the Leibniz-Institut für Polymer forschung Dresden e.V. is gratefully acknowledged.

REFERENCES

1. Murty V. M.; De, S. K. *Rubber Chem. Technol.* **1982**, *55*, 287.
2. Lopattananon, N.; Jitkalong, D.; Seadan, M. *J. Appl. Polym. Sci.* **2011**, *120*, 3242.
3. Gomina, M.; Pinot, L.; Moreau, R.; Nakache, E. In Fracture of Polymers, Composites and Adhesives II 32; European Structural Integrity Society Publication, Elsevier Ltd.: Oxford, United Kingdom, **2003**; p 399.
4. Rajeev, R. S.; Bhowmick, A. K.; De, S. K.; Bandyopadhyay, S. *J. Appl. Polym. Sci.* **2003**, *90*, 544.
5. Rajeev, R. S.; Bhowmick, A. K.; De, S. K.; Kao, G. J. P.; Bandyopadhyay, S. *Polym. Comp.* **2002**, *23*, 574.
6. Kashani, M. R. *J. Appl. Polym. Sci.* **2009**, *113*, 1355.
7. Iijima, S. *Nature* **1991**, *354*, 56.
8. Dresselhaus, M. S.; Dresselhaus, G.; Eklund, P. C. In Science of Fullerenes and Carbon Nanotubes: Their Properties and Applications; Academic Press: San Diego, CA, **1996**; p 756.
9. Oberlin, A.; Endo, M.; Koyama, T. *J. Cryst. Growth.* **1976**, *32*, 335.
10. Baughman, R. H.; Zakhidov, A. A.; de Heer, W. A. *Science* **2002**, *297*, 787.
11. White, A. A.; Best, S. M.; Kinloch, I. A. *Int. J. Appl. Ceram. Technol.* **2007**, *4*, 1.
12. Singh, M. K.; Shokuhfar, T.; Gracio, J. J. D.; de Sousa, A. C. M.; Fereira, J. M. D.; Garmestani, H.; Ahzi, S. *Adv. Funct. Mater.* **2008**, *18*, 694.
13. Hortiguela, M. J.; Gutierrez, M. C.; Aranaz, I.; Jobbagy, M.; Abarrategi, A.; Moreno-Vicente, C.; Civantos, A.; Ramos, V.; Lopez-Lacomba, J. L.; Ferrer, M. L.; del-Monte, F. *J. Mater. Chem.* **2008**, *18*, 5933.
14. Ci, L.; Suhr, J.; Pushparaj, V.; Zhang, X.; Ajayan, P. M. *Nano. Lett.* **2008**, *8*, 2762.
15. Subramoney S., *Adv. Mater.* **1998**, *10*, 1157.
16. Salvetat, J. P.; Briggs, G. A. D.; Bonard, J. M.; Bacsa, R. R.; Kulik, A. J.; Stockli, T.; Burnham, N. A.; Forro, L. *Phys. Rev. Lett.* **1999**, *82*, 944.
17. Yao, C. H.; Manas-Zloczower, I. *Polym. Eng. Sci.* **1996**, *36*, 305.
18. Kim, Y. A.; Hayashi, T.; Endo, M.; Gotoh, Y.; Wada, N.; Seiyama, *J. Sci. Mater.* **2006**, *54*, 31.
19. Mahmood, N.; Khan, A. U.; Ali, Z.; Khan, M. S.; Haq, A. U.; Stockelhuber, K. W.; Gohs, U.; Heinrich, G. *J. Appl. Polym. Sci.* **2012**, *123*, 3635.
20. Kabir, M. E.; Saha, M. C.; Jeelani, S. *Mater Sci Eng: A.* **2007**, *459*, 111.
21. Maiti, S.; De, S. K.; Bhowmick, A. K. *Rubb. Chem. Technol.* **1992**, *65*, 293.
22. Wu, D. F.; Zhang, Y. S.; Zhang, M.; Yu, W. *Biomacromolecules* **2009**, *10*, 417.
23. Sharifi, S.; Kamali, M.; Mohtaram, N. K.; Shokrgozar, M. A.; Rabiee, S. M.; Atai, M.; Imani, M.; Mirzadeh, H. *Polym. Adv. Technol.* **2011**, *12*, 605.